Mechatronics and Intelligent Transportation Systems
https://www.acadlore.com/journals/MITS

Influence of Electromagnet-Rail Coupling on Vertical Dynamics of EMS Maglev Trains

Yougang Sun[1,2*], Dinggang Gao[2], Zhenyu He[1], Haiyan Qiang[3]

[1] Institute of Rail Transit, Tongji University, 201804 Shanghai, China
[2] National Maglev Transportation Engineering R&D Center, Tongji University, 201804 Shanghai, China
[3] Logistics Engineering College, Shanghai Maritime University, 201306 Shanghai, China

[*] Correspondence: Yougang Sun (1989yoga@tongji.edu.cn)

Received: 08-10-2022 **Revised:** 09-12-2022 **Accepted:** 10-01-2022

Citation: Y. G. Sun, D. G. Gao, Z. Y. He, and H. Y. Qiang, "Influence of electromagnet-rail coupling on vertical dynamics of EMS maglev trains," *Mechatron. Intell Transp. Syst.*, vol. 1, no. 1, pp. 2-11, 2022. https://doi.org/10.56578/mits010102.

Abstract: Active control is essential for EMS maglev trains to achieve stable suspension. Currently, the main line's suspension performs well, but in areas with low track stiffness, such as the garage, turnouts, and other lines, unexpected coupling vibration is more likely to occur. Control parameters, vehicle parameters, and rail parameters are all closely related to this phenomenon. In this study, the vehicle-rail coupling dynamic equation with secondary suspension system is first established, and used to disclose the effects of different parameters on the electromagnet-rail coupling vibration of the EMS maglev train. Next, the authors adopted the proportional-derivative (PD) controller, and proposed the concept of maglev train control frequency. Next, a general simulation model was established based on the MATLAB/Simulink, and numerical simulation was carried out to reveal how the secondary suspension frequency, the control frequency and the rail frequency affect the electromagnet-rail coupling vibration. The research results provide a reference for the design of maglev trains, controllers, and tracks, laying a theoretical basis for the maintenance of maglev commercial lines.

Keywords: Maglev train; Vehicle-rail coupling; Second system suspension; Control frequency; Track frequency

1. Introduction

With the advantages of minimal friction, better turning capability, faster potential speeds, and environmental friendliness, maglev transportation technology has advanced quickly in recent decades [1-3]. Maglev transit will be extremely successful in the near future as a result of people's unrelenting desire of travel speed and comfort. Currently, the only commercial maglev train (Figure 1) is the EMS train. One of the fundamental elements of maglev transportation is the magnetic levitation technology. The rail, secondary suspension, and suspension control system are essential for ensuring that maglev vehicles operate to the highest standards [4].

(a) Incheon line (b) Changsha line (c) Shanghai line (d) Emsland line

Figure 1. EMS maglev transportation line

The EMS modeling is at a fairly advanced stage. The model parameters, however, are difficult to get and will change as the vehicle operates. The model also exhibits considerable nonlinearity and is susceptible to disturbance, which complicates the controller design. The conventional magnetic levitation control method, such as PID controller, and state feedback controller, is created based on the linearization model close to the equilibrium point.

These techniques can change the air gap, but they have limited ability to deal with parameter changes or disturbances when the system state is far from the equilibrium point. The air gap of EMS maglev train is about 8.5 mm. Therefore, the train will collide with the rail as a result of the performance decline of levitation control, creating significant safety issues.

The suspension mechanism of the EMS maglev train requires real-time feedback control of the suspension gap, making it simple to input extra energy and produce vibration in the vehicle rail coupling. The vehicle-rail coupling vibration will have a negative impact on passenger comfort as well as increase the risk of a train collision and other major safety issues. The algorithm for suspension control and vehicle-rail coupling vibration are interdependent. To achieve sable levitation, researchers from over the globe have recently presented a range of magnetic levitation control algorithms. The FDW (frequency domain weighting) approach and LQR levitation controller were integrated by MacLeod and Goodall [5] to increase their ability to control the influence of rail irregularity. To address parameter change and nonlinearity, Sinha and Pechev [6] introduced a model reference adaptive controller (MRAC), and used an evaluation function for the optimization of the airgap error. With sliding mode control and neural-fuzzy switching law, Sun et al. [7] created an adaptive Neural-Fuzzy Robust Controller that can suppress the influence of external interference and have smooth control inputs. When the train is stationary on the track, Li et al. [8] introduced a levitation control law with a virtual energy harvester to eliminate the unexpected oscillation for maglev vehicle and track. To reduce vibration caused by the vehicle-rail coupling, Sun et al. [9] developed a dynamic model of the maglev train-track coupling with flexible track and designed a feedback controller based on fuzzy logic. Additionally, with the development of AI (artificial intelligence), numerous intelligent control algorithms have started to be investigated in the field of magnetic levitation systems, including neural networks [10-12], genetic algorithms [13, 14], support vector machines [15], Monte Carlo simulation [16], and so on. These control algorithms, however, cannot completely guarantee the eradication of vibration caused by vehicle-track coupling. The reason is that it is unclear how the vehicle-track coupling vibration is affected by the track, secondary suspension, and control system collectively.

This study establishes and analyzes the nonlinear mathematical model of train-track coupling dynamics. Then, simulations and analyses were performed on the influence laws of secondary suspension frequency, maglev track frequency, and control system frequency.

2. Vehicle-Track Coupling Dynamics Modeling

There are two general technical approaches to investigate the relationship and dynamics of magnetic tracks. One is to develop the vehicle's dynamics model and magnetic-track interaction using commercial dynamic software (e.g., SIMPACK and UM). The alternative is to build the magnetic track relationship using a reduced mathematical model between single point suspension and track coupling. The latter method's mathematical model makes it more practical for controller design and stability study. Moreover, it is easier to investigate the relationship and law of magnetic orbit when system parameters are changed quantitatively. This paper uses the second modeling approach.

Figure 2 depicts a simplified representation of the magnetic-track relationship for a medium-low speed maglev train.

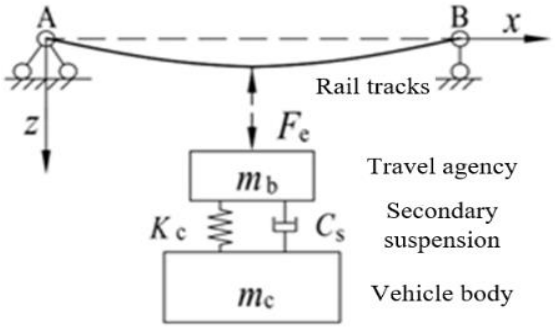

Figure 2. Model of magnetic track relationship

The dynamics model of vehicle body and electromagnet can be expressed as [17-19]:

$$\begin{cases} m_c \ddot{z}_c = m_c g - F_s \\ m_b \ddot{z}_b = m_b g + F_s - F_e \\ F_s = K_s(z_c - z_b) + C_s(\dot{z}_c - \dot{z}_b) \end{cases} \tag{1}$$

where, m_c is the body mass; m_b is the mass of the electromagnet.

The track equation can be expressed as:

$$\ddot{q}_n(t) + 2\zeta_n w_n \dot{q}_n + w_n^2 q_n = p_n \tag{2}$$

where, ζ_n is the damping ratio; w_n is the natural frequency of the n-th mode:

$$\zeta_n = \frac{c_g}{2m_g w_n}; w_n = \sqrt{\frac{EI}{m_g}}(\frac{n\pi}{L})^2; p_n = C_{gn}F_e \tag{3}$$

where, m_g is the mass of track per linear meter; c_g is the damping coefficient of the track; E is the elastic modulus of the track; I is the moment of inertia of the track; F_e is the electromagnetic force acting on the track.

The electromagnetic force can be expressed as:

$$F_e = \frac{\mu_0 N^2 A}{4}\left(\frac{i}{\delta}\right)^2 = \mathrm{K_f}\left(\frac{i}{\delta}\right)^2 \tag{4}$$

Eq. (4) is subjected to Taylor expansion at the nominal operating point:

$$F_{ed} = C_i \cdot i_d - C_\delta \cdot \delta_d$$

where, $C_i = \frac{\mu_0 N^2 A I_0}{2\delta_0^2}$; $C_\delta = \frac{\mu_0 N^2 A I_0^2}{2\delta_0^3}$; i_d, δ_d and F_{ed} are the current, voltage, floating gap and electromagnetic force after linearization, respectively.

Combining Eq. (1), the linearized model of the suspension subsystem can be obtained as:

$$\begin{cases} m_c \ddot{z}_c = -F_s \\ m_b \ddot{z}_b = F_s - F_{ed} \\ F_s = K_s(z_c - z_b) + C_s(\dot{z}_c - \dot{z}_b) \end{cases} \tag{5}$$

The PD control law can be expressed as:

$$\begin{cases} i_d = K_p e_d + K_d \dot{e}_d \\ e_d = \delta_d - q(t) - \delta_{ref} \end{cases} \tag{6}$$

where, $q(t)$ is the vertical displacement of the track; δ_{ref} is the target gap.

The dynamic equation of the suspension system can be expressed as

$$(m_b + m_c)\ddot{\delta}_d + C_i K_d \dot{\delta}_d + (C_i K_p - C_\delta)\delta_d = F_p \tag{7}$$

where, F_p is the external interference.

It can be seen from the above equation that K_p and K_d have obvious physical significance. The suspension stiffness and damping of the system can be changed by adjusting K_p and K_d, respectively. The values of these parameters depend on the damping and frequency features of the system, provided that the system meets certain stability and robustness requirements.

According to the dynamic equation of the suspension subsystem, the characteristic frequency f_n of the control system can be defined as:

$$f_n = \frac{1}{2\pi}\sqrt{\frac{C_i K_p - C_\delta}{m_b + m_c}} \quad , \quad \xi_n = \frac{c_n}{2(m_b + m_c)w_n} = \frac{c_i k_d}{4\pi(m_b + m_c) f_n}$$

The suspension frequency damping of the secondary system can be expressed as:

$$f_n = \frac{1}{2\pi}\sqrt{\frac{K_s}{m_c}}; \xi_n = \frac{c_s}{2m_c w_s}$$

The first-order frequency and damping of the track can be expressed as:

$$\zeta_n = \frac{c_g}{2m_g w_n}; w_n = \sqrt{\frac{EI}{m_g}}(\frac{\pi}{L})^2$$

A vehicle- track coupling dynamics model with two-system suspension was established in Matlab/Simulink. The values of relevant parameters of the vehicle are displayed in Table 1.

Table 1. Vehicle parameters

Physical quantity	Numerical value
Electromagnet equivalent mass m	450 kg
Equivalent mass of vehicle body m^2 (AW0)	550 kg
Equivalent mass of vehicle body m^2 (AW3)	1,200 kg
Stiffness of secondary air spring	9.6e3 N.mm
Secondary damping	1,500 N·s/m

The control parameters are displayed in Table 2.

The calculation ranges of the gap feedback coefficient and speed feedback coefficient are 1,100~51,000 and 70~1,020, respectively. The general calculation is 10,000 and 370.

Table 2. Control parameters

Linearized current coefficient	Ci	768.3553
Linearized clearance factor	Cδ	2621448

3. Influence of Secondary Suspension Frequency

The vehicle was assumed as empty, the track section was set to 26.1m, and the gap feedback coefficient and speed feedback coefficient were configured as 10,000 and 370, respectively. The system parameters are displayed in Table 3.

The original stiffness of air spring (9.6e4 N/m) was multiplied by 0.5, 1, 1.5 and 2, respectively, to change the suspension frequency of the secondary system.

Table 3. System parameters

Physical parameter	Parameter 1	Parameter 2	Parameter 3	Parameter 4
Air spring stiffness	4.8e4 N/m	9.6e4 N/m	1.44e5 N/m	1.92e5 N/m
f_s	1.4868	2.1	2.5753	2.9736
Damping ratio	0.1	0.1	0.1	0.1

Figure 3 and Figure 4 summarize the simulation results.

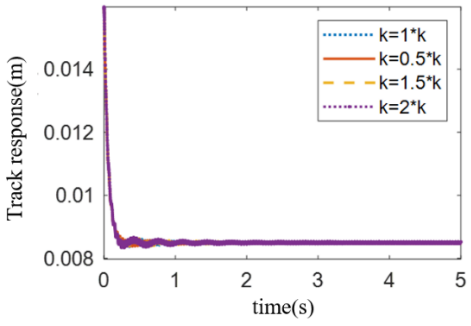

(a)

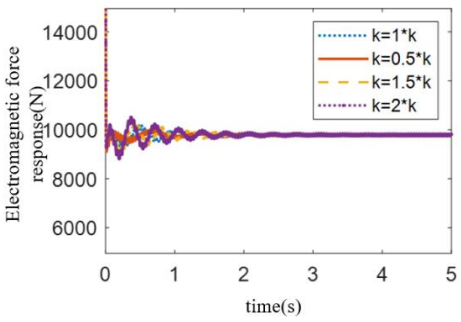

(b)

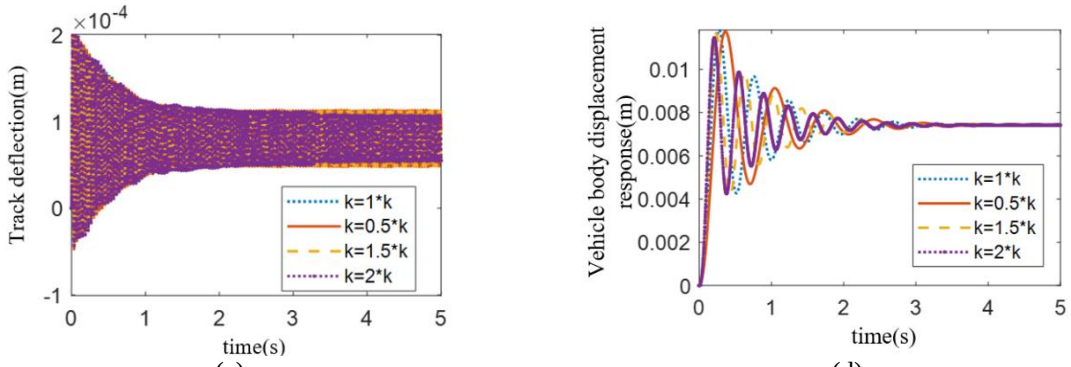

(c) (d)

Figure 3. Influence law of two-system suspension frequency

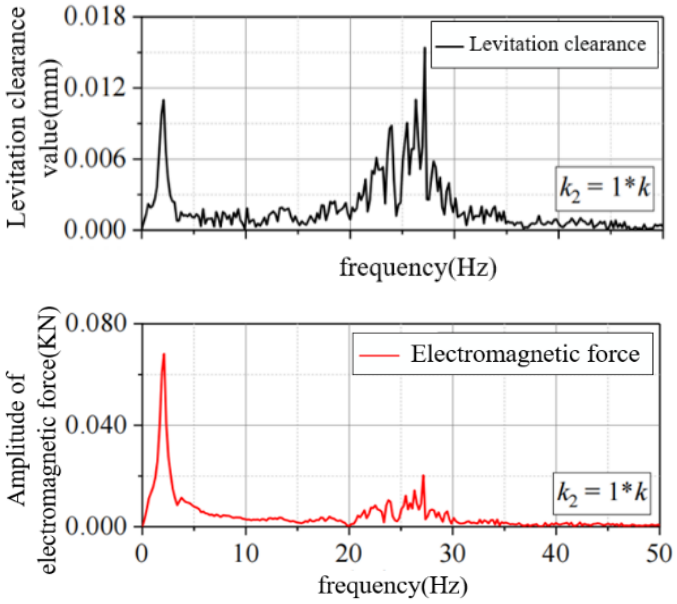

(a) Suspension clearance and electromagnetic force

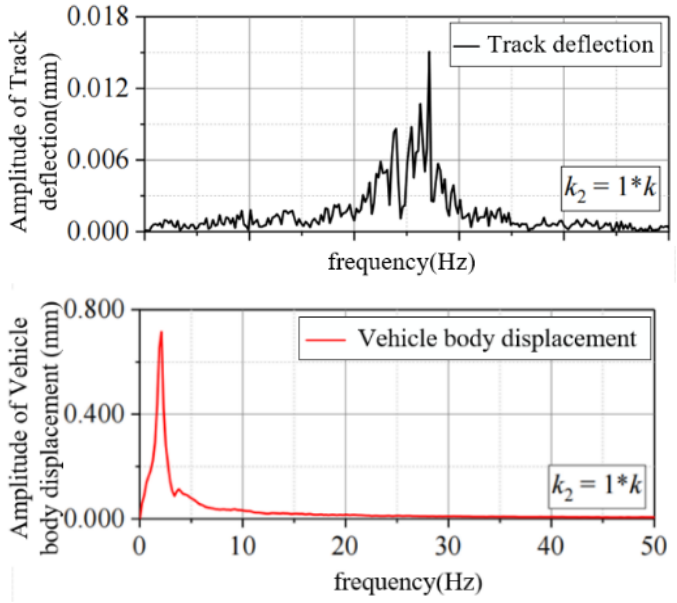

(b) Track deflection and body displacement

Figure 4. Spectrum of the original two-system stiffness

According to Figure 3 and Figure 4, the track beam vibrates mostly at a natural frequency of 26.1 Hz, with the amplitude being less affected by the stiffness of the secondary suspension. The frequency at which the car body vibrates increases in direct proportion to the stiffness of the secondary suspension, which also affects the suspension gap and the adjustment amplitude of the suspension current.

4. Influence of Control Frequency

The vehicle was assumed to be empty and the track frequency was set to 7 Hz.

4.1 Influence of k_p

The control frequency was changed by multiplying k_p with 0.5, 1, 2, and 3, respectively. The specific values after the change are displayed in Figure 5 and Figure 6.

As shown in Figure 5 and Figure 6, k_p has a certain effect on the vibration amplitude and convergence of the track beam. The larger the k_p, the greater the relative amplitude of the track beam vibration. With the growing k_p, the suspension gap converges to the target position faster. In addition, the larger the k_p, the smaller the fluctuation of the suspension gap.

4.2 The Influence of k_d

For the no-load condition, the track frequency was selected as 7 Hz, the secondary system suspension frequency as 2.1 Hz, and the control frequency as 11.3 Hz. The initial value k_d of 370 was multiplied by 0.2, 0.5, 1, and 2 respectively to change the control system damping. Figure 7 records the response of suspension clearance and electromagnetic force, as well as the response of track deflection and vehicle displacement.

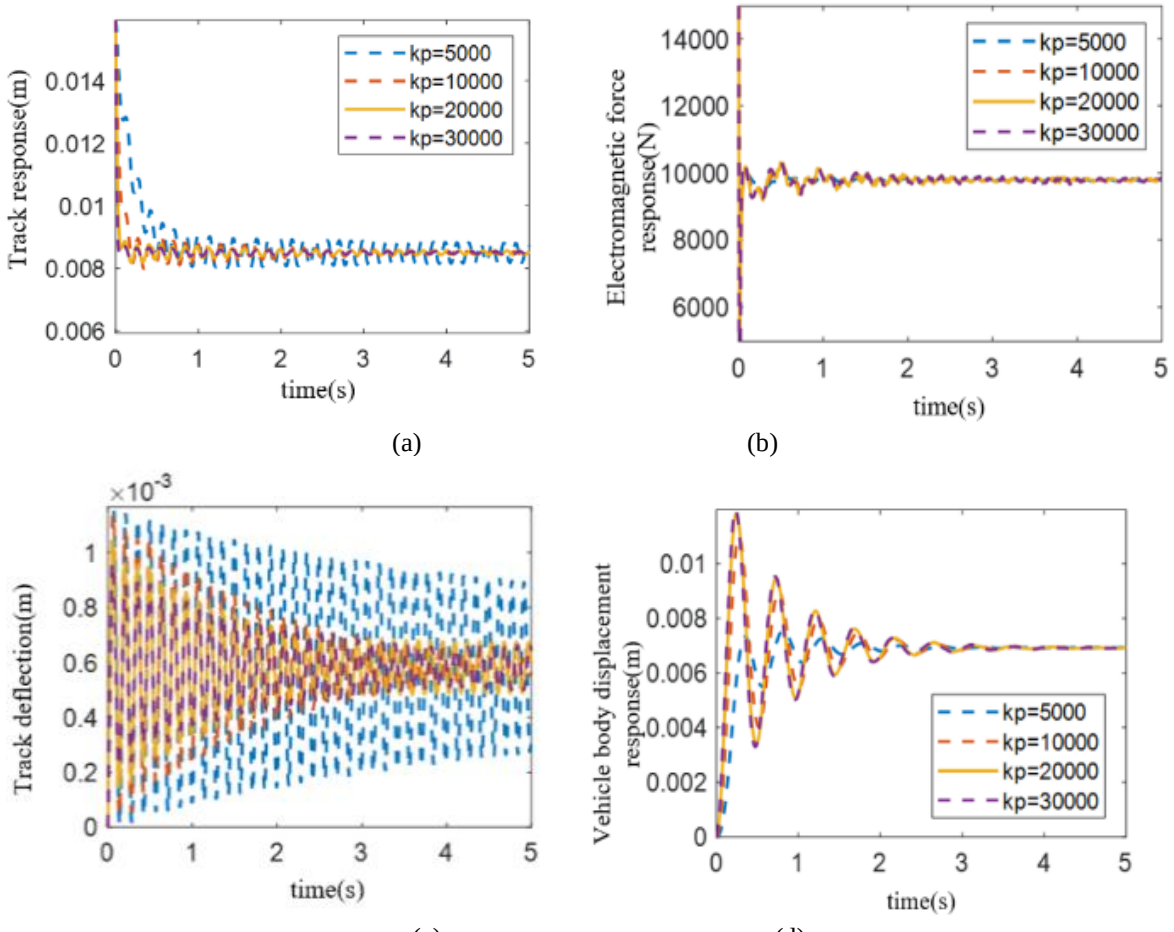

Figure 5. Influence law of k_p

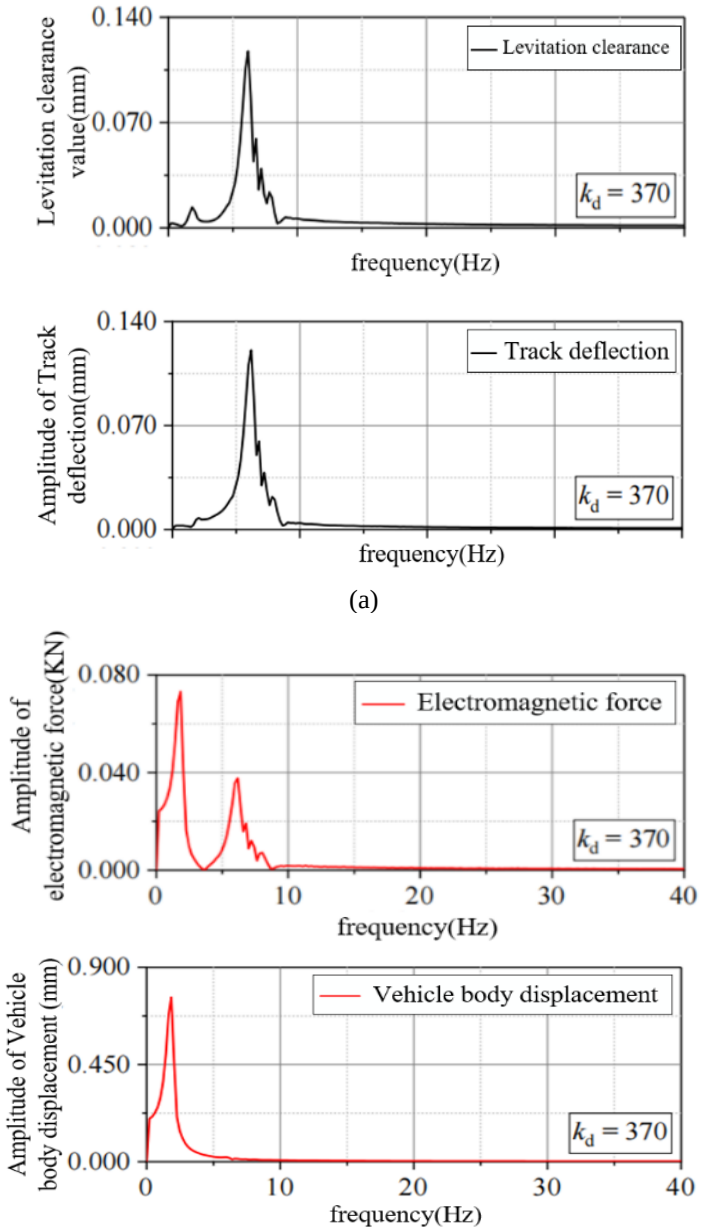

Figure 6. Response spectrum (*kp* = 10,000)

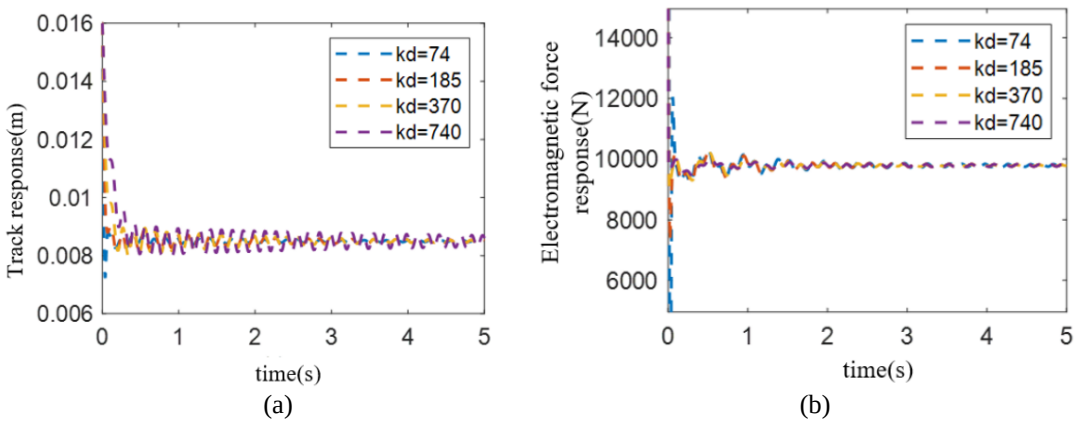

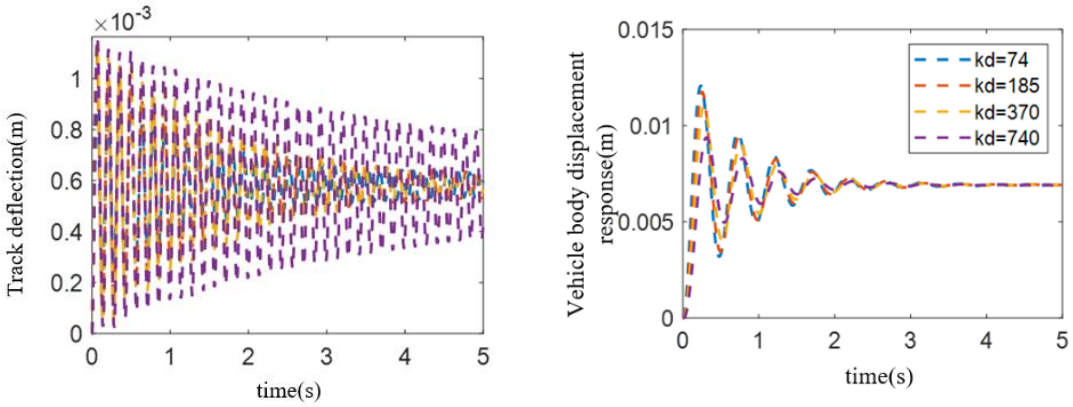

(c) (d)

Figure 7. The influence law of k_d

It can be seen from Figure 7 that the larger the k_d, the better the convergence of vehicle body vibration. With the growing value of k_d, it takes a longer time for the maglev to reach the equilibrium position for the first time. When k_d arrives at 740, the suspension gap fluctuates the most. When k_d is small, the damping of the system is insufficient, and the electromagnetic force fluctuates greatly about the equilibrium position.

5. Influence of Orbital Frequency

The vehicle was assumed to be empty, the track length was set to 26.1m, and the gap feedback coefficients and speed feedback coefficients were configured as 10,000 and 370, respectively.

The first-order frequencies of the track are displayed in Table 4.

Table 4. First-order frequencies of the track

	1	2	3	4	5
Frequency Hz	7	15	20	26.1	39.15
Remark	**Concrete**	**Unsupported 1**	**Unsupported 2**	**Turnout level 1**	**1.5*26.1**

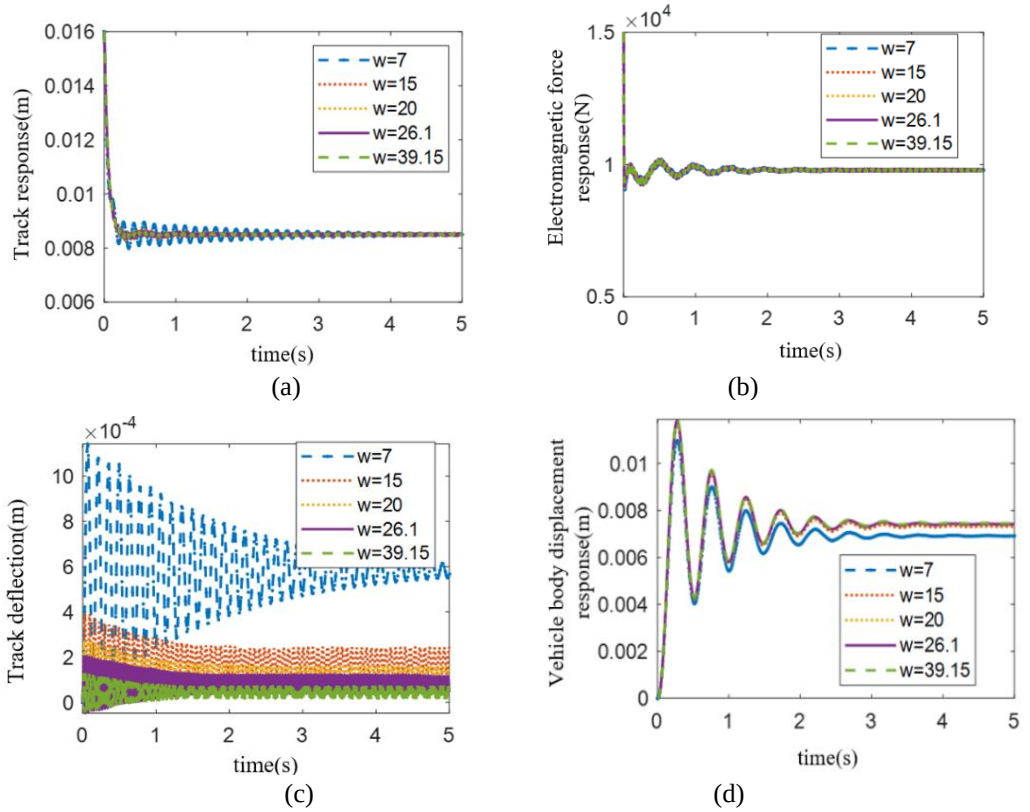

(a) (b)

(c) (d)

Figure 8. Law of influence of track frequency

As shown in Figure 8, the natural frequency is primarily responsible for the track beam's vibration. Since the track beam's stiffness controls how its natural frequency changes, the lower the bending stiffness of the beam with a low natural frequency, the more the track beam's equilibrium point shifts and the more dynamic vibration amplitude is during the vibration process.

6. Conclusions

In this study, the equation for the dynamics of the maglev vehicle-rail coupling with two-system suspension is established, using the multi-body dynamics approach, electromagnetic theory, and control theory. The analytical model is created using MATLAB software, before performing simulation analysis. The following are the primary conclusions:

(1). The stiffness of the secondary suspension has less of an impact on the track beam's amplitude, and the vibration attenuation is gradual. The secondary suspension frequency determines how the vehicle vibrates. The frequency of vehicle body vibration increases with secondary suspension stiffness, and the convergence speed with respect to track beam vibration increases.

(2). The dynamic amplitude of vehicle body vibration is not significantly impacted by the secondary suspension stiffness. The vibration of the track beam and the car body both have an impact on the suspension gap and suspension current, with the vibration of the vehicle body having the greatest impact on the electromagnetic force.

(3). The secondary system's suspension stiffness improves, along with the adjustment amplitude of suspension clearance and suspension current.

(4). As k_p rises, the suspension gap fluctuates less and convergence occurs more quickly, but the relative amplitude of the track beam's vibration rises. When k_d is low, the system's damping is insufficient, which causes the electromagnetic force to fluctuate a lot near its equilibrium position.

(5). The displacement deviation of the track beam's equilibrium point and the amplitude of the dynamic vibration during the vibration process are all higher for a beam with a low natural frequency than for a beam with a higher bending stiffness.

Data Availability

The data used to support the findings of this study are available from the corresponding author upon request.

Conflicts of Interest

The authors declare that they have no conflicts of interest.

References

[1] H. W. Lee, K. C. Kim, and J. Lee, "Review of maglev train technologies," *IEEE T. Magn.*, vol. 42, no. 7, pp. 1917-1925, 2006. https://doi.org/10.1109/TMAG.2006.875842.

[2] L. Yan, "Development and application of the maglev transportation system," *IEEE T. Appl. Supercon.*, vol. 18, no. 2, pp. 92-99, 2008. https://doi.org/10.1109/TASC.2008.922239.

[3] J. Wang, S. Wang, and J. Zheng, "Recent development of high temperature superconducting maglev system in China," *IEEE T. Appl. Supercon.*, vol. 19, no. 3, pp. 2142-2147, 2009. https://doi.org/10.1109/TASC.2009.2018110.

[4] I. Boldea, L. N. Tutelea, W. Xu, and M. Pucci, "Linear electric machines, drives, and MAGLEVs: An overview," *IEEE T. Ind. Electron.*, vol. 65, no. 9, pp. 7504-7515, 2019. http://dx.doi.org/10.1109/TIE.2018.2889580.

[5] C. MacLeod and R. M. Goodall, "Frequency shaping LQ control of maglev suspension systems for optimal performance with deterministic and stochastic inputs," *IEE P-Contr. Theor. Ap.*, vol. 143, no. 1, pp. 25-30, 1996. https://doi.org/10.1049/IP-CTA:19960057.

[6] P. K. Sinha and A. N. Pechev, "Model reference adaptive control of a maglev system with stable maximum descent criterion," *Automatica*, vol. 35, no. 8, pp. 1457-1465, 1999. https://doi.org/10.1016/S0005-1098(99)00040-0.

[7] Y. Sun, J. Xu, H. Qiang, and G. Lin, "Adaptive neural-fuzzy robust position control scheme for maglev train systems with experimental verification," *IEEE T. Ind. Electron.*, vol. 66, no. 11, pp. 8589-8599, 2019. https://doi.org/10.1109/TIE.2019.2891409.

[8] J. H. Li, J. Li, D. Zhou, P. Cui, L. Wang, and P. Yu, "The active control of maglev stationary self-excited vibration with a virtual energy harvester," *IEEE T. Ind. Electron.*, vol. 62, no. 5, pp. 2942-2951, 2015. https://doi.org/10.1109/TIE.2014.2364788.

[9] Y. G. Sun, J. Q. Xu, H. Y. Qiang, W. J. Wang, and G. B. Lin, "Hopf bifurcation analysis of maglev vehicle-

guideway interaction vibration system and stability control based on fuzzy adaptive theory," *Comput. Ind.*, vol. 108, pp. 197-209, 2019. https://doi.org/10.1016/j.compind.2019.03.001.
[10] R. J. Wai and J. D. Lee, "Adaptive fuzzy-neural-network control for maglev transportation system," *IEEE T. Neural. Networ.*, vol. 19, no. 1, pp. 54-70, 2008. https://doi.org/10.1109/TNN.2007.900814.
[11] S. J. Wu, C. T. Wu, and Y. C. Chang, "Neural-Fuzzy gap control for a current/voltage-controlled 1/4-vehicle maglev system," *IEEE T. Intell. Transp.*, vol. 9, no. 1, pp. 122-136, 2008. https://doi.org/10.1109/TITS.2007.911353.
[12] Y. G. Sun, J. Q. Xu, G. B. Lin, and N. Ning, "Adaptive neural network control for maglev vehicle systems with time-varying mass and external disturbance," *Neural. Comput. Appl.*, vol. 2021, pp. 1-12. https://doi.org/10.1007/s00521-021-05874-2.
[13] S. Kusagawa, J. Baba, K. Shutoh, and E. Masada, "Multipurpose design optimization of EMS-type magnetically levitated vehicle based on genetic algorithm," *IEEE T. Appl. Supercon.*, vol. 14, no. 2, pp. 1922-1925, 2004. https://doi.org/10.1109/TASC.2004.830933.
[14] C. Q. Ye, G. T. Ma, K. Liu, and J. S. Wang, "Intelligent optimization of an HTS maglev system with translational symmetry," *IEEE T. Appl. Supercon.*, vol. 26, no. 4, pp. 1-5, 2016. https://doi.org/10.1109/TASC.2016.2519280.
[15] C. Liu and G. Rong, "SVM order inverse system decoupling time-varying sliding mode control of double suspension systems of machining center," China Mech. Eng., vol. 26, no. 5, pp. 668-674, 2015. http://dx.doi.org/10.3969/j.issn.1004-132X.2015.05.018.
[16] G. Zhang, J. Zhang, H. L. Zhang, Q. T. Meng, and M. Fan, "Calculation and verification of magnetic force in a radial permanent magnetic bearing based on quasi-monte Carlo method," In 2020 IEEE 1st China International Youth Conference on Electrical Engineering, Wuhan, China, November 1-4, 2020, IEEE, pp. 1-5. https://doi.org/10.1109/CIYCEE49808.2020.9332684.
[17] Y. Sun, J. Xu, G. Lin, W. Ji, and L. Wang, "RBF neural network-based supervisor control for maglev vehicles on an elastic track with network time delay," *IEEE T. Ind. Inform.*, vol. 18, no. 1, pp. 509-519, 2022. https://doi.org/10.1109/TII.2020.3032235.
[18] W. Hu, Y. Zhou, and Z. Zhang, "Model predictive control for hybrid levitation systems of maglev trains with state constraints," *IEEE T. Veh. Technol.*, vol. 70, no. 10, pp. 9972-9985, 2021. https://doi.org/10.1109/TVT.2021.3110133.
[19] Y. Sun, J. Xu, H. Wu, G. Lin, and S. Mumtaz, "Deep learning based semi-supervised control for vertical security of maglev vehicle with guaranteed bounded airgap," *IEEE T. Intell. Transp.*, vol. 22, no. 7, pp. 4431-4442, 2021. https://doi.org/10.1109/TITS.2020.3045319.